Optics & Laser Technology 166 (2023) 109562

Contents lists available at ScienceDirect

Optics and Laser Technology

journal homepage: www.elsevier.com/locate/optlastec

Full length article

Ultralong passively mode-locked ring fibre lasers in the femtosecond range assisted by Raman amplification

Inés Cáceres-Pablo [a], Francesca Gallazzi [b], Fernando Solís [a], Pedro Corredera [a], Juan Diego Ania-Castañón [a]

[a] Instituto de Óptica "Daza de Valdés", IO-CSIC, Serrano 121, 28006 Madrid, Spain
[b] Photonics Laboratory, Tampere University, Korkeakoulunkatu 3, 33720, Finland

ARTICLE INFO

Keywords:
Ultrashort high-energy pulse generation
Mode-locked fiber oscillator
Ultralong-ultrafast ring fiber lasers (UURFL)
Raman amplification
Time-Stretched Dispersive Fourier Transform (TS-DFT)
Erbium Doped Fiber Amplifier (EDFA)
Semiconductor saturable absorber mirror (SESAM)

ABSTRACT

A novel fibre ring laser architecture reliant on the use of Raman-assisted nonlinearity management over ultralong cavities is used for the first time to generate ultrashort pulses in ring resonators of up to 25.2 km. Using this approach, stable generation of pulses under 200 fs with estimated maximum energies of the order of μJ and an ultra-low repetition rate of 20 kHz is reported in passively mode-locked ultra-long ring fibre lasers of 10 km, overcoming previous limitations to pulse duration imposed by dispersive effects. The proposed system operates in the telecommunications infrared C-band, and relies on an Erbium-doped fibre amplifier, a polarization-insensitive InN-based semiconductor saturable absorber mirror and standard telecommunication fibres, and does not require external amplification or compression stages. Real-time monitoring of the output signal through the time-stretch dispersive Fourier transform technique shows that the average laser optical spectrum corresponds to that of the individual pulses. The presented devices constitute a new family of ultrafast fibre oscillators with unique characteristics suited for a broad range of applications.

1. Introduction

The extraordinary potential of ultrashort pulse lasers has led, over the past few decades, to the successful exploration of a myriad of applications in areas as varied as medicine, telecommunications, metrology, spectroscopy, materials processing and energy research, as well as to the recognition of some seminal advances in the field with awards as prestigious as the Nobel Prize itself. The experimental foundations of the field of ultrafast optics can be traced back to the pioneering work on mode-locking in solid-state lasers carried out by Demaria et al. [1], shortly followed by the generation of sub-picosecond pulses in organic dye lasers by Shank and Ippen [2]. In parallel, the theoretical foundations for the field were being laid by researchers such as Haus and New during the 70′s and 80′s [3,4]. The critical contribution of chirped-pulse amplification in 1985 [5] became the key to unlock applications with high-energy requirements, and started a new era of widespread use of ultrashort pulse technologies. The field has continued to be intensely active, with constant technological advances coming through in quick succession from areas such as materials science, nanophotonics or system design.

Passively mode-locked optical fibre ring resonators have deservedly garnered particular attention since the early 90′s [6,7] among the laser configurations capable of ultrafast pulse generation. Self-starting mode-locking is a convenient feature that can be facilitated through the use of a ring configuration and the introduction of some form of saturable absorber in the cavity [8], leading to the production of very short pulses. These sources display the usual characteristics of fibre lasers, such as stability, efficiency, compactness, easy integrability, are nearly maintenance-free and allow for convenient output beam handling, which makes them highly attractive. Despite the aforementioned advantages, their applicability is still restricted in certain areas, mostly due to limited achievable pulse energy and peak power, which in practice has been limited to the few hundreds of kW for pulses in the range of a few hundred fs. This constraint has hindered their direct use in power-demanding materials processing or industrial solutions, where other options, such as solid-state lasers, dominate.

A range of alternatives, such as nonlinear polarization rotation [9], semiconductor saturable absorbing mirrors [10] (SESAMs) or nonlinear optical loop mirrors [11], are available to generate pulses in the fs range through self-starting mode-locking in fibre ring resonators, but maximum pulse energy is limited by the fundamental barrier set by the accumulation of nonlinear phase, which generally leads to the break-up

E-mail address: ines.caceres@csic.es (I. Cáceres-Pablo).

https://doi.org/10.1016/j.optlastec.2023.109562
Received 1 March 2023; Received in revised form 27 April 2023; Accepted 29 April 2023
Available online 7 June 2023

of pulses due to the combined action of Kerr nonlinearity and chromatic dispersion [12]. A potential way of avoiding such energy limitations could be found by exploiting the dissipative soliton resonance (DSR) effect [13,14], but unfortunately this approach leads to the generation of long-duration pulses due to the accumulation of chirp. Similarly, pulsed variations of the well-known continuous wave (CW) ultra-long fibre laser sources [15–18] have been proposed [18–21] to increase pulse energy by reducing repetition rate, but the considered architectures have been incapable of generating pulses shorter than a few ns [18] due to dispersive effects.

Thus, although recent times have seen the development of passively mode-locked fibre lasers capable of reaching moderately high peak powers through the use of photonic crystal fibre, ring fibre lasers have been generally regarded as excellent seeds for high power pulse generation in combination with additional stages based on techniques such as chirped-pulse amplification and recompression, but the goal of obtaining pulses in the hundreds of fs with energies around the μJ out of a fibre master oscillator comprised of conventional communications fibre has remained elusive.

This paradigm began to shift recently with our demonstration [22] of a new family of multi-km ring lasers capable of producing stable sub-250 fs pulses with peak powers in excess of the MW and repetition rates below the MHz. This novel ultralong-ultrafast ring fibre laser architecture (UURFL) makes use of InN-based SESAMs [23], and combines two distinctive propagation regimes through the management of gain, loss and dispersion, so the signal propagates as an adiabatic fundamental soliton along most of the cavity length and then as a gain-guided pulse as it is amplified in a short section of erbium-doped fibre amplifier (EDFA). Please note that although polarization effects such as non-linear polarization rotation [9] may occur in sections of our setup, the system does not include polarizing or polarization dependent elements. The utilized InN-SESAM is itself polarization independent, and the non-polarized pulses are not affected by polarization dependent gain in the Raman-amplified extended section. Relying for the most part on low-cost and readily available telecommunication fibres and components, this family of lasers presents a rich potential that we have only begun to explore, as their low repetition rates, combined with the high energy of the pulses, makes them uniquely suited for the generation of record-density frequency comb supercontinua, such as the one that we have recently applied to the spectroscopic detection of pollutants in the atmosphere [24].

In this manuscript we take the original concept of the UURFL a step further, by proposing and demonstrating the possibility of using the Raman effect [25] to induce adiabatic soliton transmission conditions over much longer sections of the ring, enabling a dramatic reduction of the corresponding fundamental mode repetition rate while preserving pulse duration. This approach clears a new path to take UURFL performance to new limits in terms of achievable pulse energy and power.

Precise management of power and thus nonlinearities inside the extended cavity is critical for ultralong ring fibre lasers to obtain stable mode-locking at fs regimes. As shown in [22] for rings of up 2.4 km, this can be achieved by carefully adjusting signal power after the SESAM, so pulse peak power at the input of the section of standard single-mode fibre (SSMF) was always close to that of a fundamental soliton, allowing for stable ultrashort pulse propagation over a few km. Although some pulse breathing inevitably takes place, the comparison between the pulses at the input and output of the SSMF confirms how the pulse profile adapts adiabatically to that of fundamental soliton over short fibre lengths, without being affected by dispersive broadening.

Pulse attenuation in longer ring lengths, on the other hand, led to pulse broadening (see Fig. 1a) and the loss of mode locking. Please note that the system is designed so that pulse propagation through the ring takes place at moderate to low energies, except in the final steps of the EDFA prior to the laser output.

In order to extend cavity length while ensuring that the system still supports stable mode-locking with ultrashort pulse generation, the conditions for fundamental soliton propagation must be guaranteed for a longer cavity. In this regard, virtually lossless distributed Raman amplification using, for example, cavity ultra-long Raman fibre lasers [15–17] (URFLs) has been demonstrated to support adiabatic, close-to-ideal soliton transmission over many soliton periods through SSMF [26] (see Fig. 1b). Moreover, a precise enough cancellation of local attenuation, achievable even for distances over 50 km, preserves soliton properties, including soliton interaction, and can be efficiently described analytically using rather straightforward soliton perturbation theory [27]. Thus, it follows that the introduction of an independently amplified section of fibre operating in conditions as close as possible to transparency could, in principle, be used to extend ring length while preserving ultrashort pulse support.

2. Experimental setup

Our proposed new high-power ultrafast ring fibre laser architecture is represented in Fig. 2. The system presents anomalous average dispersion, thanks to a multi-km extended cavity long section of standard telecommunications fibre. The laser [22] includes a 16 m EDFA operating with a non-adjustable gain level at a fixed output saturated power of 24 dBm at 1560 nm. A polarization-insensitive InN-based SESAM resistant to high irradiances [1–3], with a fast response capable of producing pulses in the order of the hundreds of fs in standard, short ring cavities [23], is used to achieve passive mode-locking. The SESAM section is a free space configuration coupled to the fibre system through a circulator. Total losses in the SESAM section can be manually controlled by adjusting the focus of the laser beam out of the fibre and the spot size incident to the mirror. This allows us to manually adjust the power entering the extended cavity without the need of an additional attenuator prior to the circulator, to ensure pulse peak powers close to fundamental soliton condition.

To complete the experimental scheme, standard off-the shelf components (relying on telecommunication optical SSMF) are employed; an

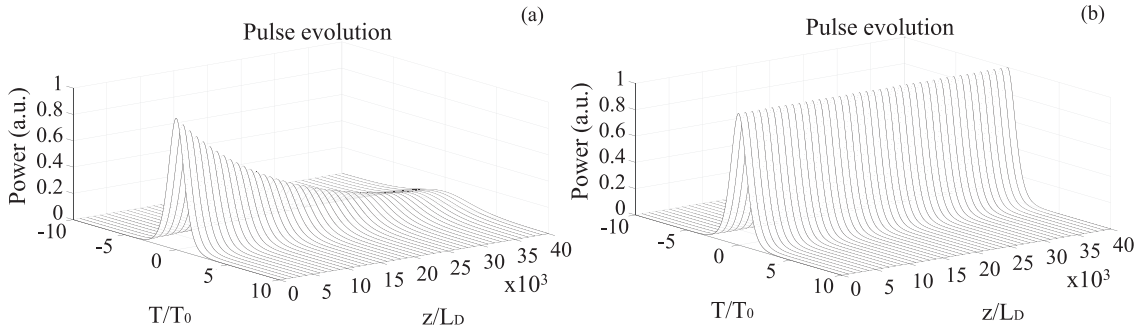

Fig. 1. Solitonic pulse evolution. (a) Through a non-amplified fibre. (b) Through a virtually losssless one. L_D represents dispersion length, which for 200 fs pulses in standard transmission fibre takes the value of $L_D \approx 0.65$ m.

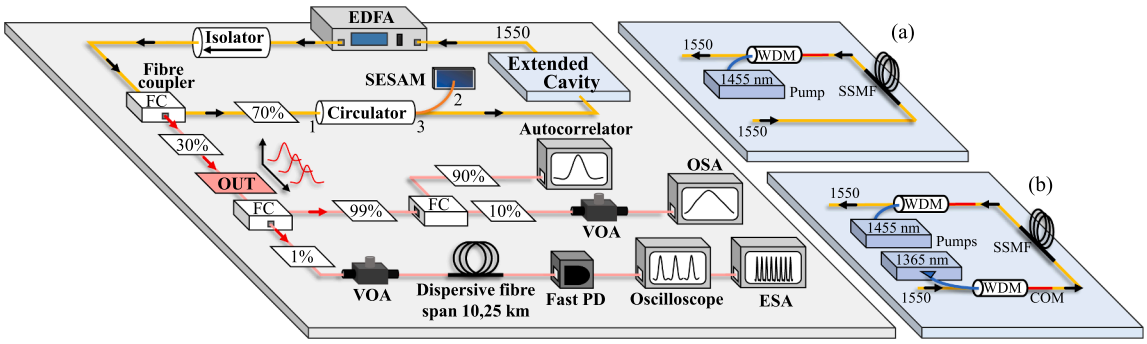

Fig. 2. Schematic of the setup for the characterization of ultralong pulsed fibre lasers, where the extended cavity can take two different configurations, depending on the selected distributed amplification solution. (a) Raman-amplified extended cavity design for the 5.4 km. and 10 km rings. (b) Raman-amplified extended cavity design for the 25.2 km ring. The operation of the laser is counter-clockwise.

isolator located after the EDFA to guarantee unidirectionality in the propagation through the cavity, a 70–30 % coupler that provides the ring laser output through the 30 % port, and the extended cavity, which in the explored implementations can comprise a 5.4 km, 10 km or 25.2 km spool of ITU G.652 SSMF inserted after the SESAM.

Output pulses obtained at 1.56 μm are analyzed simultaneously with the autocorrelator, the optical spectrum analyzer (OSA), the electrical spectrum analyzer (ESA) and the power meter to measure the full width at half maximum (FWHM), the center wavelength, the repetition rate and the average power. Finally, single pulses are recorded using the time-stretched dispersive Fourier Transform (TS-DFT) technique [28], for which the output signal of the laser is attenuated to a linear regime, and propagated through a 10.25 km spool of ITU G.652 fibre, so the pulses spread temporally under the effect of dispersion and are converted from femtosecond to nanosecond pulses. The broadened signal is then directed to a high-speed, low-noise 25 GHz photodetector and recorded in a real-time oscilloscope.

Ultralong ring laser designs assisted by two different Raman amplification schemes are compared. Option Fig. 2a is a 1st-order counter-propagating Raman amplification scheme with a pump centered at 1455 nm and it is used for the cavity lengths of 5.4 km and 10 km, whereas option Fig. 2b is a 2nd-order bidirectional scheme with a counter-propagating pump centered at 1455 nm that is itself pumped by another beam at 1365 nm co-propagating with the ring laser signal and it is employed for the 25.2 km length cavity.

To guarantee adiabatic soliton transmission we optimize the Raman pumping scheme by monitoring and minimizing low-signal power excursion at 1550 nm with an optical time-domain reflectometer over the amplified extended cavity for all considered ring lengths. Thus, we will refer to the configurations that minimize power excursion as "optimal" in the sense that they provide the closest conditions for quasi-lossless transmission in the extended fiber section.

2.1. Optimization of the amplification scheme

Although 2nd-order amplification offers the best gain distribution, power excursion in the 5.4 km and 10 km cavities can be made negligible using the simpler scheme Fig. 2(a). On the other hand, for the 25.2 km cavity, we find that the best results are obtained with scheme Fig. 2(b), which is the only one that allows for self-starting and fully stable mode locking.

As can be seen from Figs. 3, 4 and 5, numerical simulations offer excellent agreement with the experiment, and allow us to precisely determine the optimal configuration for each fibre ring.

Please note that although the results presented below are obtained for lasers relying on an InN material SESAM, the possibility of extending ring length through Raman-assisted adiabatic soliton propagation could be potentially applied to pulsed fibre lasers employing different saturable absorbers, including artificial ones [29], as well as diverse laser

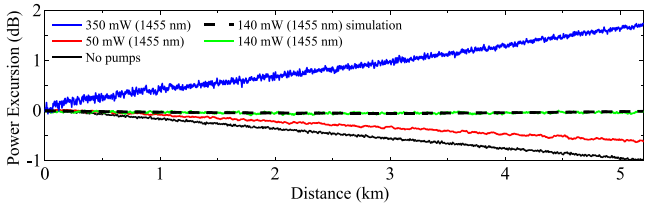

Fig. 3. Signal power evolution in the 5.4 km extended fibre section for different pumping values using amplifier configuration Fig. 2a. The dashed lines represent the optimal solutions determined through numerical simulations.

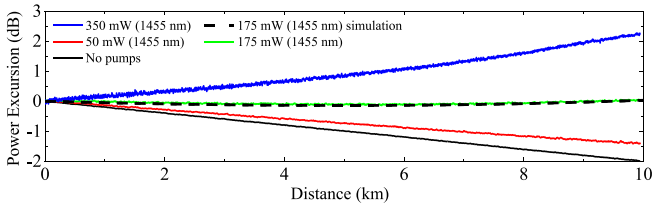

Fig. 4. Signal power evolution in the 10 km extended fibre section for different pumping values using amplifier configuration Fig. 2a. The dashed lines represent the optimal solutions determined through numerical simulations.

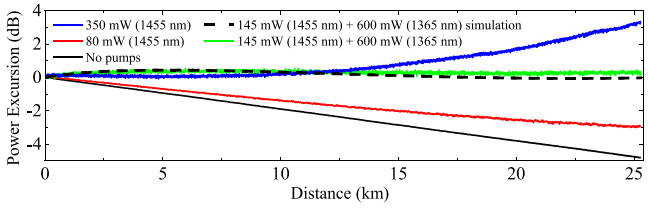

Fig. 5. Signal power evolution in the 25.2 km extended cavity fibre section using amplifier configurations Fig. 2a and Fig. 2b. The dashed lines represent the optimal solutions determined through numerical simulations.

architectures. Artificial saturable absorbers could present certain advantages, including very long life times and broad availability, but nevertheless, systems relying on such solutions would require a separate optimization, and often involve additional complexities, such as the precise handling of polarization.

3. Results

3.1. Mode locking in the 5.4 km and 10 km configurations

The amplification schemes tested above allow us to extend cavity

length while maintaining average output power, potentially reducing repetition rate and increasing pulse energy. In the case of the 5.4 km and 10 km rings, power adjustment prior to the extended cavity and the use of the optimized distributed Raman gain profiles (see Figs. 3 and 4.) allows us to achieve fundamental mode-locking (FML) with repetition rates of 36,7 kHz and 20 kHz. Pulses display autocorrelation traces with FWHM between 155 fs in the 5.4 km ring and 200 fs in 10 km ring directly out of the master oscillator, which would translate to pulse durations between 100 fs and 110 fs for the shorter case, and between 130 fs and 141 fs for the longer one, assuming that pulse shape is somewhere between a soliton and a Gaussian [22].

For these lengths, mode-locking is also achievable, with precise adjustment of input signal power, for amplifier configurations other than the optimal, since power excursion is not high, in some instances even with no pumping. In the optimally amplified cases, immediate self-starting mode-locking is achievable as soon as the EDFA is turned on, whereas when the system is not amplified, it is hardly achievable and highly unstable, particularly for the 10 km ring, even at constant room temperature.

Fig. 6a displays autocorrelation traces for the 5.4 km ring, whereas Fig. 6b and 6c compare the measured output laser spectrum with the individual pulse profiles obtained in a real-time oscilloscope after attenuation and dispersive broadening. As expected from the TS-DFT, the real-time profile of each pulse in the oscilloscope qualitatively reflects the optical spectrum of the laser, minus the noise component generated at about 1530 nm in the EDFA, the EDFA's peak emission wavelength, which contains less than a 6 % of the output energy. Fig. 6d displays the RF spectrum, with the corresponding repetition frequency, measured after the TS-DFT section.

Fig. 7 displays the obtained results for the 10 km extended ring, which are qualitatively similar to those obtained for the shorter cavity. Please note that both in the 5.4 km and in the 10 km rings, we observe that slight overamplification leads to shorter pulses, as the pulse adiabatically adapts to a fundamental soliton of slightly higher power. This happens at the expense of additional noise and reduced stability, which are more evident in the 10 km case, but implies that an amplification system optimized for slightly positive gain might offer best performance in some applications than one optimized for quasi-lossless transmission. As before, the real-time profile of each broadened pulse in the oscilloscope qualitatively reflects the optical spectrum of the laser, minus the noise component centered at 1530 nm representing less than 6 % of the total energy contained in the laser spectrum for the optimally amplified case. Maximum pulse energy inside the ring, immediately after the EDFA, estimated directly from the average output power and repetition rate, is of the order of 2,05 μJ for 5.4 km and 3.21 μJ for 10 km, corresponding to output pulse energies after the 30 % splitter of 0.615 μJ for 5.4 km and 0.963 μJ for 10 km".

3.2. Mode locking in the 25.2 km configuration

When using the extended 25.2 km ring, mode-locking was not attainable without distributed amplification. In this case, while scheme Fig. 2a allowed for the obtention of pulsed regimes, only scheme Fig. 2b allowed us to achieve stability during extended periods of time thanks to its flatter profile and reduced noise. Even in the optimal amplifier configuration, mode-locking is only possible to the 4th harmonic and above, leading to repetition rates of 32 kHz or higher. The limit case of the 4th harmonic is illustrated in Fig. 8. Fig. 8a displays autocorrelation traces and Fig. 8b the spectra at the output of the 25.2 km ring for two different pumping configurations, namely the minimum pumping required to observe some sort of lock-in, and the optimal virtually lossless transmission that leads to stable output. Fig. 8c and 8d display the individual pulse traces overlay and the RF spectrum with the corresponding repetition frequency, respectively, after TS-DFT for optimal amplification.

The inset in Fig. 8b displays the optical spectrum of the laser when the Raman pumps are turned off, leading to noisy CW operation at a central wavelength of approximately 1530 nm. By increasing backward pump power at 1455 nm to 120 mW and adjusting focus and losses at the SESAM we are able to achieve lock-in to the 4th harmonic, with 321 fs FWHM autocorrelation traces (pulse duration between 208 fs and 227 fs) and a broad optical spectrum centered at 1560 nm which nevertheless displays a very visible noise component at 1530 nm. Switching to bi-directional pumping and optimally adjusting pump power for quasi-lossless propagation in the extended cavity allows for a reduction of the noise and autocorrelation FWHM of 300 fs (pulse duration between 194 fs and 212 fs), a broadened spectrum and stable pulsed operation over several hours with identical periodic pulses.

Mode locking to the 6th harmonic (48 kHz) is also achievable in the 25.2 km configuration by adjusting focus and losses at the SESAM. The results for this case are summarized in Fig. 9, where autocorrelation traces corresponding to different distributed amplification configurations are compared (Fig. 9a), as well as the resulting output spectra (Fig. 9b), pulse traces overlay (Fig. 9c) and RF spectrum (Fig. 9d). The noticeable tilt in Fig. 8c and 9c could be attributed to accumulated third order dispersion [30].

As with the 4th harmonic case, optimizing gain distribution in the extended cavity leads to shorter pulses (with a minimum autocorrelation FWHM of 260 fs, or pulse duration between 169 fs and 184 fs), broader and cleaner spectra and highly stable operation over extended periods of time.

Table 1. collects the obtained results for the different configurations studied and available regimes of operation, including continuous wave operation and lock-in to different harmonics. From the table, the increasing relevance of distributed amplification for longer cavities becomes apparent, to the point that no mode locking is achievable in the longer cavity configuration without a minimum reduction of power

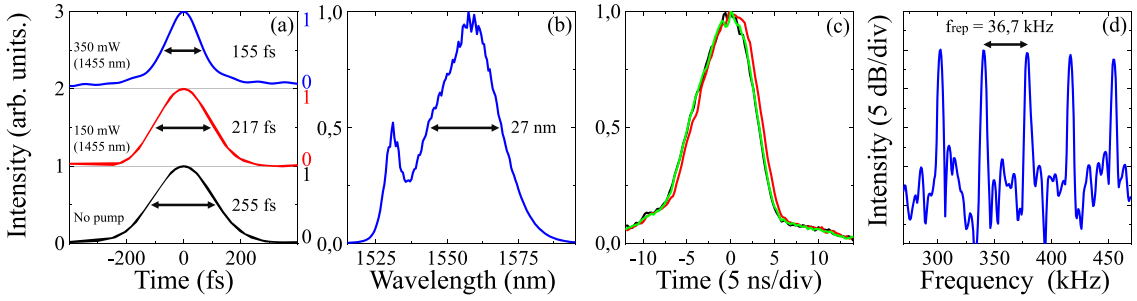

Fig. 6. Traces for the output pulsed signal in three amplifier configurations for the 5.4 km laser, for an under amplified configuration, optimized quasi-lossless transmission and slightly over-amplified transmission with stable mode-locking to the 1st harmonic (repetition rate 36,7 kHz). (a) Autocorrelation traces. (b) Optical spectrum for the optimally amplified case. (c) Individual broadened pulse traces overlay after the TS-DFT section for the optimally amplified case. (d) RF spectrum. The curves are shifted vertically for better readability.

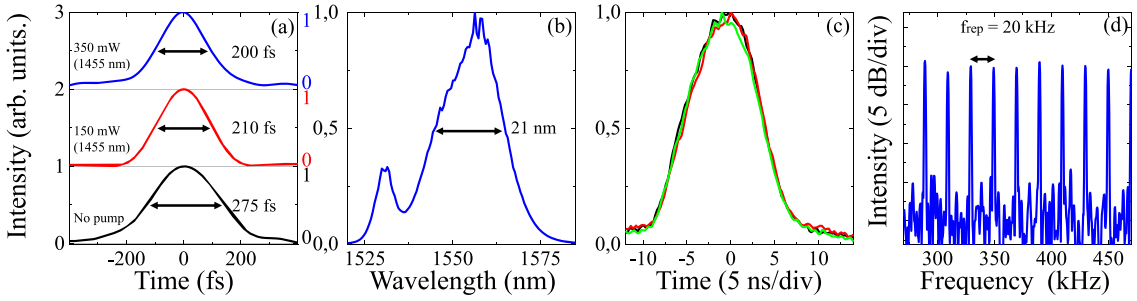

Fig. 7. Traces for the output pulsed signal in three amplifier configurations for the 10 km laser, for an under amplified configuration, optimized quasi-lossless transmission and slightly over-amplified transmission with stable mode-locking to the 1st harmonic (repetition rate 20 kHz). (a) Autocorrelation traces. (b) Optical spectrum for the optimally amplified case. (c) Individual broadened pulse traces overlay after the TS-DFT section for the optimally amplified case. (d) RF spectrum. The curves are shifted vertically for better readability.

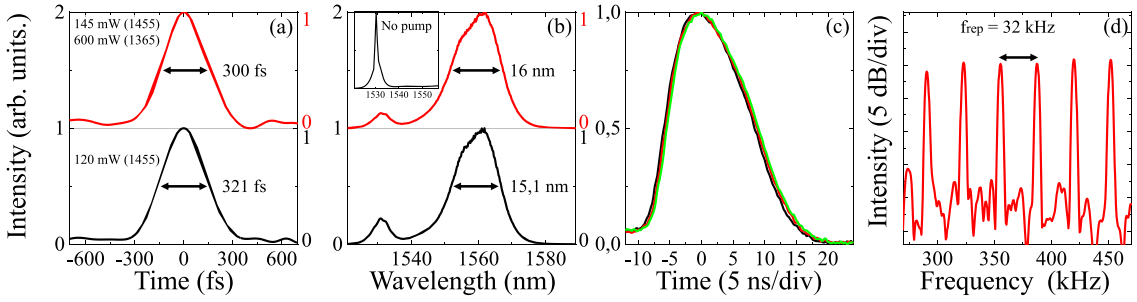

Fig. 8. Traces for the output pulsed signal in the 25.2 km laser, for an under amplified configuration and optimized quasi-lossless transmission, with stable mode-locking to the 4th harmonic (repetition rate 32 kHz). (a) Autocorrelation traces. (b) Output spectrum of the laser for the two pumping cases under consideration (inset - no pumping). (c) Individual broadened pulse traces overlay after the TS-DFT section with optimal distributed amplification. (d) RF spectrum. The curves are shifted vertically for better readability.

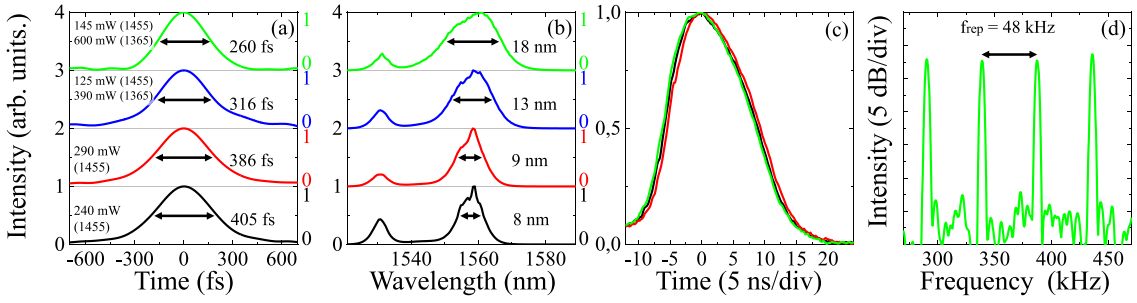

Fig. 9. Traces for the output pulsed signal in the 25.2 km laser, for an under amplified configurations and optimized quasi-lossless transmission, with stable mode-locking to the 6th harmonic (repetition rate 48 kHz). (a) Autocorrelation traces. (b) Output spectrum of the laser for the four pumping cases under consideration. (c) Individual broadened pulse traces overlay after the TS-DFT section with optimal distributed amplification. (d) RF spectrum. The curves are shifted vertically for better readability.

excursion to guarantee adiabatic soliton transmission.

In order to ensure that pulse energy is not overestimated due to the presence of interpulse radiation, the last column in the table shows the output pulse energy after the 30 % splitter calculated from the average of the integration of individual pulse profiles in the oscilloscope, taking into account the photodiode's conversion gain and the losses in the TS-DFT line. Although this alternative method yields a slightly lower estimation of pulse energy, of approximately an 84 % of the value obtained directly from dividing average power by repetition rate, it nevertheless provides additional confirmation that most of the laser output energy is contained in the individual pulses.

4. Conclusion

To summarize, the presented results incontrovertibly demonstrate the possibility of using distributed Raman amplification to extend cavity length in fibre ring lasers while maintaining the necessary quasi-lossless transmission conditions for the support of ultrashort pulse generation. This approach unlocks the potential of the recently proposed ultralong-ultrafast ring fibre lasers, effectively giving birth to a new family of optical oscillators producing pulses with durations in the hundreds of fs at telecommunication wavelengths, and inherently low repetition rates of the order of the tens of kHz, which leads to estimated output energies of the order of several μJ. This estimation is close to the expected self-focusing limit for the used fibre, signal wavelength and pulse duration, which suggests any relevant further improvement in output energy must come from a modification in one of these factors.

In our study, and using InN-SESAMs, minimum repetition rates and pulse energies are obtained for moderate length rings of 10 km, for which fundamental mode-locking is achievable through our proposed

Table 1
Results for the different configurations studied and available regimes of operation. Maximum pulse energy is the estimated energy after EDFA amplification calculated from average power and repetition frequency. Output pulse energy (a) corresponds to pulse energy after the 30 % coupler, estimated from average power and repetition frequency. Output pulse energy (b) reflects the calculated pulse energy after the 30 % coupler, from direct integration of the broadened pulse profiles in the scope, taking into account the photodiode's conversion gain and the losses in the line.

Ring configuration (km)	Raman counter pump (mW)	Raman co pump (mW)	Autocorrelation trace FWHM (fs)	Spectral width at FWHM (nm)	Repetition frequency (kHz)	Maximum pulse energy (μJ)	Output pulse energy (a) (nJ)	Output pulse energy (b) (nJ)
5.4	0	0	255	16.4	36.7	1.70	510	427
5.4	150	0	217	19.6	36.7	1.86	558	468
5.4	350	0	155	27	36.7	2.05	615	516
10	0	0	275	15.3	20	2.74	822	689
10	150	0	210	19.4	20	3.11	932	782
10	350	0	200	21	20	3.21	964	808
25.2	0	0	–	–	–	–	–	–
25.2	120	0	321	15.1	32	2.05	616	517
25.2	145	600	300	16	32	2.13	640	537
25.2	240	0	405	8	48	1.22	366	306
25.2	290	0	386	9	48	1.23	369	310
25.2	125	390	316	13	48	1.37	411	345
25.2	145	600	260	18	48	1.42	427	358

nonlinearity management approach. Longer lengths of 25 km are shown to offer easier harmonic mode switching, being of particular interest in applications requiring repetition rate tunability, and illustrating the broad potential of this new family of laser.

Author contributions. J.D.A.C. conceived the study. I.C.P., F.G., P. C., and J.D.A.C performed the experimental measurements; I.C.P., F.S. and J.D.A.C. carried out the numerical simulations; I.C.P. and J.D.A.C. analyzed the results and wrote the initial draft. All authors contributed to the discussion and reviewed the manuscript.

Funding. This work was funded by Ministerio de Ciencia, Innovación y Universidades (grants RTI2018-097957-B-C33 - ECOSYSTEM and PID2021-128000OB-C21 - PRECISION) and Comunidad de Madrid – Fondos FEDER (S2018/NMT-4326, SINFOTON2-CM).

Declaration of Competing Interest

The authors declare that they have no known competing financial interests or personal relationships that could have appeared to influence the work reported in this paper.

Data availability

All data underlying the results presented in this paper are available in the main text.

Acknowledgments

The authors wish to thank Prof. E. Monroy for providing the InN samples employed in the SESAM and Profs. F. B. Naranjo, M. González-Herráez and J.M. Soto-Crespo for their useful comments.

Appendix A. Methods and materials

A.1. Experimental design

Our experiment aimed to prove the possibility of using optimized Raman amplification to assist in the management of nonlinearities in ultra-long mode-locked fibre ring lasers, without negatively impacting pulse duration or characteristics. In order to achieve this, signal power is greatly reduced after the SESAM stage, prior to the Raman amplified section, in order for the individual pulses to converge to soliton propagation conditions. Inside the long amplified section, minimal signal variation is sought. After propagating through the extended, Raman-assisted section, the signal undergoes amplification inside the EDFA (please refer to Fig. 2b) and is extracted from the laser through a splitter. Full experimental characterization of the output signal is provided through a number of methods, including direct autocorrelation, optical spectral analysis, as well as real-time pulse analysis through TS-DFT and the monitoring of the converted RF spectrum.

A.2. Physical principles and basic theory

The well-known steady-state equations governing the evolution of average signal power inside the second-order Raman distributedly amplified section [15] are:

$$\frac{dP^{\pm}_{R_1}}{dz} = \mp\alpha_1 P^{\pm}_{R_1} \mp g_{R_{12}}\frac{\nu_1}{\nu_2}P^{\pm}_{R_1}\left(P^{+}_{R_2}+P^{-}_{R_2}+4h\nu_2\Delta\nu_2\left(1+\frac{1}{e^{h(\nu_1-\nu_2)/K_BT}-1}\right)\right)\pm\varepsilon_1 P^{\mp}_{R_1} \tag{1}$$

$$\frac{dP^{\pm}_{R_2}}{dz} = \mp\alpha_2 P^{\pm}_{R_2} \pm g_{R_{12}}\left(P^{\pm}_{R_2}+2h\nu_2\Delta\nu_2\left(1+\frac{1}{e^{\frac{h(\nu_1-\nu_2)}{K_BT}}-1}\right)\right)\left(P^{+}_{R_1}+P^{-}_{R_1}\right)\mp g_{R_{2S}}\frac{\nu_1}{\nu_2}P^{\pm}_{R_2}\left(P^{+}_{S}+P^{-}_{S}+4h\nu_S\Delta\nu_S\left(1+\frac{1}{e^{\frac{h(\nu_2-\nu_S)}{K_BT}}-1}\right)\right)\pm\varepsilon_2 P^{\mp}_{R_2} \tag{2}$$

$$\frac{dP^{\pm}_{S}}{dz} = \mp\alpha_S P^{\pm}_{S} \pm g_{R_{2S}}\left(P^{+}_{R_2}+P^{-}_{R_2}\right)\left(P^{+}_{S}+2h\nu_S\Delta\nu_S\left(1+\frac{1}{e^{h(\nu_2-\nu_S)/K_BT}-1}\right)\right)\pm\varepsilon_S P^{\mp}_{S} \tag{3}$$

Where the + and - superscripts represent, respectively, forward and backward propagation, the R_1 and R_2 subscripts identify the first- and second-

order Raman pumps, and the *S* subscript identifies the output laser signal at the frequency of the EDFA, for which the backward propagating component will usually be negligible thanks to the presence of the isolator. Theν_i and $\Delta\nu_i$ denote, respectively, the corresponding frequencies and bandwidths of the first- and second-order Raman pumps, ϵ_i represents the Rayleigh backscattering coefficient and the g_{Rij} indicate the Raman gain coefficients from componentν_i to componentν_j. K_B and h are respectively Boltzmann's and Planck's constants, and T represents temperature.

The optimal pumping configuration can be determined by numerically solving the set of ODEs Eqs. (1–3) while scanning the boundary condition space to determine the optimal $P_{Ri}(0)$ and $P_{Ri}(L)$ for any specific value of $P_S(0)$, minimizing signal power excursion. From the numerical solution of $P_S(z)$ we can calculate the effective gain/loss coefficient $\alpha_{eff}(z)$ for the distributedly amplified section of the ring laser, expressed as:

$$\alpha_{eff}(z) = -\frac{dP_S^+(z)/dz}{P_S^+(z)} \tag{4}$$

Inserting this $\alpha_{eff}(z)$ term into the nonlinear Schrödinger equation describing propagation inside an optical fibre we can numerically calculate the expected behaviour of a pulse that presents conditions close to that of a soliton at $z = 0$ when travelling along the extended ring assisted by any amplifier configuration. Without Raman amplification, an unchirped secant hyperbolic pulse with power adjusted to match that of a first-order soliton at the entrance of the extended section will propagate adiabatically for a few km, but eventually broaden as loses accumulate and nonlinear effects fail to cancel out fibre dispersion (Fig. 1a). On the other hand, an ideally amplified section of fibre would allow for indefinitely long quasi-solitonic propagation without a noticeable variation of the pulse profile (see Fig. 1b).

A.3. Numerical simulations

The model presented in the previous section is solved numerically to predict signal power evolution in the extended cavity for the two different amplification configurations considered. The set of coupled nonlinear ordinary differential equations (1–3) representing average power evolution through a Raman amplified system are solved using a collocation method for two-point boundary value problems based on the well-known continuous Runge-Kutta. In particular, a variant of COLSYS/COLNEW [31]. The retrieved gain/loss coefficient obtained from equation (4) can be inserted in the Nonlinear Schrödinger equation, which is solved using the usual split-step Fourier method to simulate pulse evolution under any selected distributed amplifier configuration.

The illustrative examples in Fig. 1 correspond to a 200 fs FWHM solitonic pulse input propagating through a standard fibre with 0.2 dB/km and $\beta_2 = -20\ ps^2/km$, with and without attenuation.

A.4. Temporal and spectral signal characterization

In order to characterize the system, the output pulses obtained at 1.56 μm are analyzed simultaneously in the optical domain through a power meter, a fast autocorrelator (APE PulseCheck Autocorrelator with a Crystal module NIR/IR and an IR Photodiode detector module) and an optical spectrum analyzer (Anritsu MS9710C) through the 30 % port (the 70 % − 30 % values of fibre coupling provide the highest output power under mode-locking conditions). The signal is also characterized using the time-stretched dispersive Fourier Transform technique, TS-DFT, that allows us to observe the dispersively stretched pulses in real time in a fast oscilloscope (Infiniium 9000 Series Oscilloscope MSO9404A with a bandwidth of 4 GHz, Sample rate 10 GSamples/s and memory depth of 100 Mpts) after conversion to the electrical domain in a low-noise fast 25 GHz photodetector. The electrical signal is also routed to a radiofrequency spectrum analyzer (Spectrum Master Handheld Spectrum Analyzer Anritsu MS2712E) for fast and precise monitoring of repetition rates and mode structure.

References

[1] A.J. Demaria, D.A. Stetser, H. Heynau, Self mode-locking of lasers with saturable absorbers, Appl. Phys. Lett. 8 (1966) 174–176.
[2] C.V. Shank, E.P. Ippen, Subpicosecond kilowatt pulses from a mode-locked cw dye laser, Appl. Phys. Lett. 24 (1974) 373–375.
[3] H.A. Haus, Theory of mode locking with a fast saturable absorber, J. Appl. Phys. 46 (1975) 3049–3058.
[4] G.H.C. New, Mode-locking of quasi-continuous lasers, Opt. Commun. 6 (1972) 188–192.
[5] D. Strickland, G. Mourou, Compression of amplified chirped optical pulses, Opt. Commun. 56 (1985) 219–221.
[6] E.P. Ippen, Principles of passive mode locking, Appl. Phys. B 58 (1994) 159.
[7] F. Krausz, T. Brabec, Passive mode locking in standing-wave laser resonators, Opt. Lett. 18 (11) (1993) 888.
[8] U. Keller, et al., IEEE J. Sel. Top. Quantum Electron. 2 (1996) 435–451.
[9] E. Yoshida, Y. Kimura, M. Nakazawa, Femtosecond Erbium-doped fiber laser with nonlinear polarization rotation and its soliton compression, Jpn. J. Appl. Phys. 33 (1994) 5579.
[10] O. Okhotnikov, A. Grudinin, M. Pessa, Ultra-fast fibre laser systems based on SESAM technology: new horizons and applications, New J. Phys. 6 (2004) 177.
[11] L. Chusseau, E. Delevaque, 250-fs optical pulse generation by simultaneous soliton compression and shaping in a nonlinear optical loop mirror including a weak attenuation, Opt Lett. 19 (1994) 734–736.
[12] E. Ding, P. Grelu, J. Nathan Kutz, Dissipative soliton resonance in a passively mode-locked fiber laser, Opt. Lett. 36 (2011) 1146–1148.
[13] W. Chang, A. Ankiewicz, J.M. Soto-Crespo, and N, Akhmediev Phys. Rev. A 78 (2010), 023830.
[14] P. Grelu, W. Chang, A. Ankiewicz, J.M. Soto-Crespo, N. Akhmediev, Dissipative soliton resonance as a guideline for high-energy pulse laser oscillators, J. Opt. Soc. Am. B 27 (2010) 2336–2341.
[15] J.D. Ania-Castañón, Quasi-lossless transmission using second-order Raman amplification and fibre Bragg gratings, Opt. Express 12 (2004) 4372–4377.
[16] J.D. Ania-Castañón, T.J. Ellingham, R. Ibbotson, X. Chen, L. Zhang, S.K. Turitsyn, Ultralong Raman fiber lasers as virtually lossless optical media, Phys. Rev. Lett. 96 (2006), 023902.
[17] S.A. Babin, V. Karalekas, P. Harper, E.V. Podivilov, V.K. Mezentsev, J.D. Ania-Castañón, S.K. Turitsyn, Experimental demonstration of mode structure in ultralong Raman fiber lasers, Opt. Lett. 32 (2007) 1135–1137.
[18] S. Kobtsev, S. Kukarin, Y. Fedotov, Ultra-low repetition rate mode-locked fiber laser with high-energy pulses, Opt. Express 16 (2008) 21936–21941.
[19] I.A. Yarutkina, O.V. Shtyrina, M.P. Fedoruk, S.K. Turitsyn, Numerical modeling of fiber lasers with long and ultra-long ring cavity, Opt. Express 21 (2013) 12942–12950.
[20] M.Z. Zulkifli, K.Y. Lau, H. Kbashi, M. Yasin, M.A. Mahdi, A self-pulsing ring cavity ultra-long Raman fiber laser, Laser Phys. 28 (2018), 115104.
[21] L.A. Rodríguez-Morales, B. Ibarra-Escamilla, I. Armas-Rivera, O. Pottiez, M. V. Andrés, M. Durán-Sánchez, E.a. Kuzin, "Sub-200-kHz single soliton generation in a long ring Er-fiber laser with strict polarization control by using twisted fiber", Optics Laser Technol 126 (2020), 106068.
[22] F. Gallazzi, M. Jimenez-Rodriguez, E. Monroy, P. Corredera, M. González-Herráez, F.B. Naranjo, J.D. Ania-Castañón, Sub-250 fs passively mode-locked ultralong ring fibre oscillators, Optics Laser Technol 138 (2021), 106848.
[23] M. Jiménez-Rodríguez, E. Monroy, M. González-Herráez, F.B. Naranjo, Ultrafast Fiber Laser Using InN as Saturable Absorber Mirror, J. Lightwave Technol. 36 (11) (2018) 2175–2182.
[24] F. Gallazzi, I. Cáceres, L. Monroy, J. Nuño, C. Pulido, P. Corredera, F.B. Naranjo, M. González-Herráez, J.D. Ania-Castañón, Ultralong ring laser supercontinuum sources using standard telecommunication fibre, Optics Laser Technol. 147 (2022), 107632.
[25] J. Bromage, Raman amplification for fiber communications systems, J. Lightwave Technol. 22 (1) (Jan. 2004) 79–93.
[26] M. Alcon, A. El-Taher, H. Wang, P. Harper, V. Karalekas, J.A. Harrison, J.D. Ania-Castañón, Long-distance soliton transmission through ultralong fiber lasers, Optics Lett. 34 (2009) 3104–3106.

[27] J.D. Ania-Castañón, "Implementation of Virtually Non-dissipative Links in Optical Fibre", in Proc. SIAM Conference on Nonlinear Waves and Coherent Structures, Rome (2008).
[28] K. Goda, B. Jalali, Dispersive Fourier transformation for fast continuous single-shot measurements, Nature Photonics 7 (2013) 102–112.
[29] S. Kobtsev, Artificial saturable absorbers for ultrafast fibre lasers, Optical Fiber Technol. 68 (2022), 102764.
[30] G.P. Agrawal, Nonlinear fiber optics, Academic Press, 2012.
[31] U. Ascher, Collocation for Two-point boundary value problems revisited, SIAM J. Num. Anal. 23 (3) (1986) 596–609.